



Safety in Mines Research Advisory Committee
Final Project Report

**COL816: Develop specifications for a portable counting
seismometer to be implemented routinely in mines
underground.**

R A Lynch
(richard@issi.co.za)

ISS International Limited

June 2002

Executive Summary

The SIMRAC project COL816 investigated the feasibility of a small, independent device monitoring local seismicity and extracting similar activity information to what can be recorded by a temporary network of seismometers. To do this seismic signals from a uni-axial geophone mounted on a roof-bolt stub were continuously logged while a small seismic network simultaneously operated. Various algorithms were developed and applied to the continuous data to find the one that most closely reflected the network data. A satisfactory correspondence was found, paving the way for development of such a Counting Seismometer.



Acknowledgements

This project received enthusiastic encouragement and support from many people at Brandspruit Colliery, particularly:

David Postma

Koos Janse van Vuuren

Mickiel Jacobs

Cecil Robson

Brian Vorster

to whom I am grateful.

Andrew Tsukudu and Rudi Smith of ISS International installed, commissioned, operated and de-commissioned the seismic system for the project.

Table of Contents

| | <i>Page</i> |
|---|-------------|
| Introduction | 1 |
| Project Objectives | 1 |
| Project Site | 2 |
| Description of the Seismic Network and Discussion of Recorded Data | 3 |
| Description of the Roof-Bolt Geophone and Discussion of Recorded Data | 7 |
| Exploration of Various Triggering Algorithms | 16 |
| Comparisons between the Network and Roof-Bolt Data | 20 |
| Counting Seismometer Requirements | 24 |
| Conclusions | 25 |
| References | 25 |

Introduction

Applications of seismic monitoring in the underground coal-mining environment are not common in South Africa. This is primarily because the fast pace of mining discourages even the simple power and communications infrastructure real-time seismic systems require. Nevertheless advantages of seismic monitoring in providing pre-emptive warnings of major goafing or roof failures have been accepted. For many years before the advent of mechanisation in coal mines, lives were saved by evacuating after increased levels of cracking were audible.

The best seismic information about the state of the surrounding rock is obtained by a carefully-planned permanent network of seismometers. This data consists of a source time, location and parameters such as radiated seismic energy and inelastic co-seismic deformation, associated with each seismic event that is recorded by multiple seismic stations [GUIDE1999, Mendecki 1997]. A previous SIMRAC project [COL607] used a temporary seismic network to show that even just source time data can be useful in indicating impending rock instability. The ambitious objective of this project is to investigate whether a small self-contained device, the size of a man's hand, could provide similar seismic activity information to that recorded by a network consisting of 5 tri-axial geophones, 2 Multi-Seismometer stations, a small Personal Computer, over 2 km of cabling, a 200kg flame-proof box and mine-supplied electrical power. This small device is referred to as a Counting Seismometer in this report.

Project Objectives

The objectives of this work were as follows:

1. The Site:

Select a suitable underground coal mine expected to experience major goafing or wide-spread roof stratum failures, during stooping

2. Network Seismic Data:

Install a small, intrinsically safe seismic network to record seismic data for later processing and interpretation

3. Roof-bolt geophone seismic data:

Install a roof-bolt geophone and continuously record the seismic signals for later processing and comparison with the network data

4. Data Analysis:

Compare seismic data from the network to what was recorded by the single roof-bolt sensor and test different algorithms for differentiating genuine signatures of fracturing from mining machinery noise.

The Site

This project took place at Section 17 of Brandspruit #2 shaft colliery, near Sasolburg in South Africa. Coal mining here takes place by stooping in sub-sections. In each sub-section about 8 parallel roads are developed 30m apart. Perpendicular to this some 17 splits are developed, forming a rectangular grid. Each road and split is about 8m wide, leaving square pillars of coal 22m wide supporting the sandstone/gritstone roof stratum. These pillars are then sequentially partially extracted, leaving a weakly-supported roof span of some 200m width and increasing length. At some point the roof stratum can rupture and a goaf is observed. If the roof hangs up and goafing is only superficial at a few neighbouring sub-sections, then the potential for a major goaf in the section is great. This deep rupturing of the roof stratum over a few hundreds of meters and subsequent collapse can result in powerful damaging windblasts. Both sub-sectional and major goafs can result in the continuous miner (CM) being buried, which is both inconvenient and costly.

Figure 1 depicts Section 17 with the mining layout and sub-sections. Our site is outlined in blue, and was chosen as an area prone to a major goaf. This is because the roof was being supported by a dome-like structure over the entire section and had not goafed yet. Our sub-section was the last substantial one being mined under the dome.

The CM is electrically powered from the switch-cart, which is periodically pulled back as stooping proceeds towards it. In Figure 1 the stooping proceeds towards the bottom left. During the switch-cart relocation power to the section is interrupted.

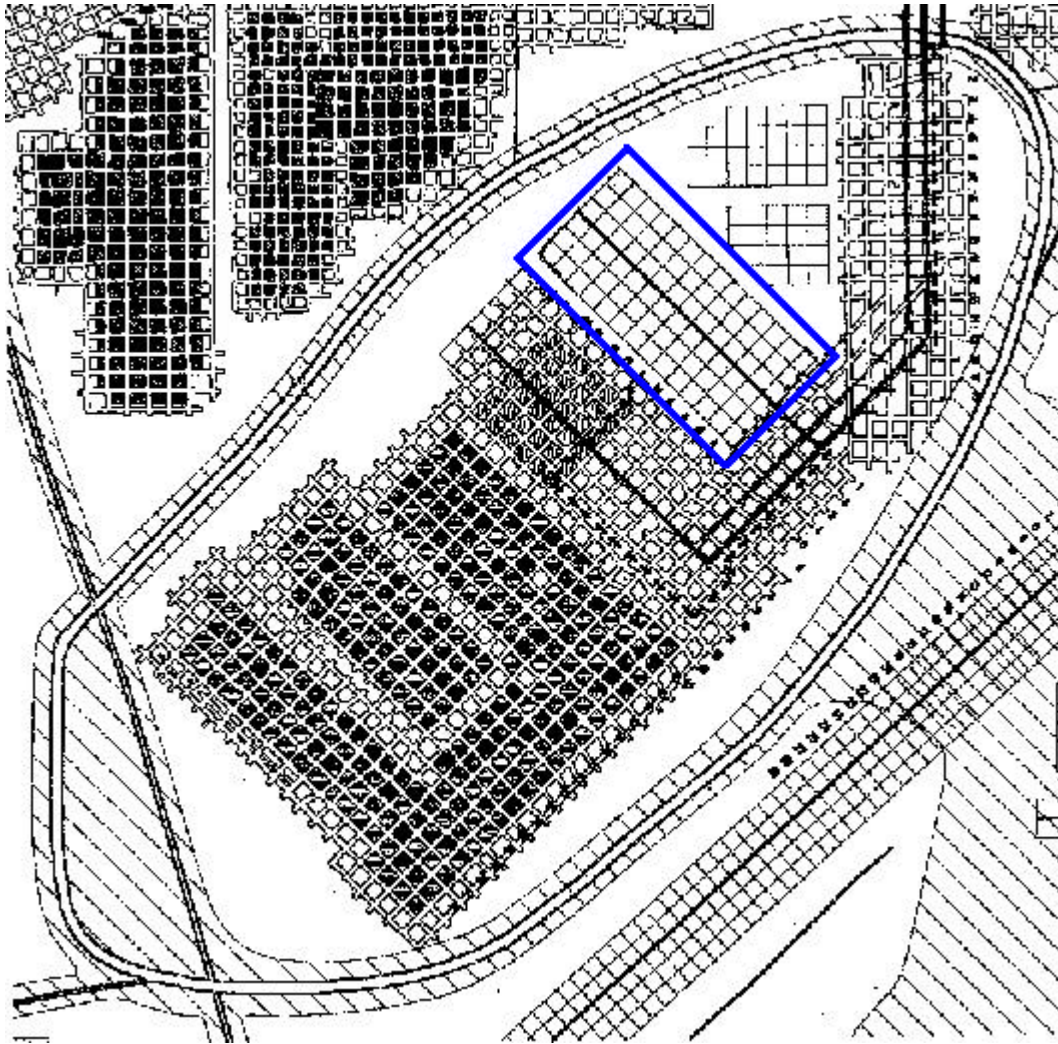


Figure 1: Map showing the stooping sub-sections of section 17. The last sub-section of the area (outlined in blue) is where this project was conducted. Black squares depict mined out pillars.

The Seismic Network

There is an understandable concern in coal mine environments about intrinsically safe equipment. Any equipment that cannot be tested and certified as such must be enclosed within a flame-proof cabinet. These enclosures are made from thick steel and are capable of withstanding an internal explosion without allowing any expulsion of flaming gas. Consequently they are very heavy and expensive. For this project the SABS tested the standard 14Hz tri-axial geophones manufactured by ISS International and certified them to be intrinsically safe. The Multi-Seismometers and communications equipment are not intrinsically safe and so were housed in a large flame-proof box of mass in excess of 200kg.

In COL607 it was shown that reasonable seismic waveforms may be obtained from using quick-set cement to create a "swallow's nest" around a geophone, acoustically coupling the geophone to the hanging wall. This method was used to grout five 14Hz tri-axial intrinsically-safe geophones in places around the stooping sub-section.

The geophones were connected by shielded instrumentation cable via barriers to the two Multi-Seismometers (MS) resident within the flame-proof box. Communications cable and barriers carry signals between the MS box and a small Personal Computer on which the Run Time System (RTS) software operates. This computer was situated in a fresh-air area about 500m from the MS box underground. The network configuration is given in Figure 2.

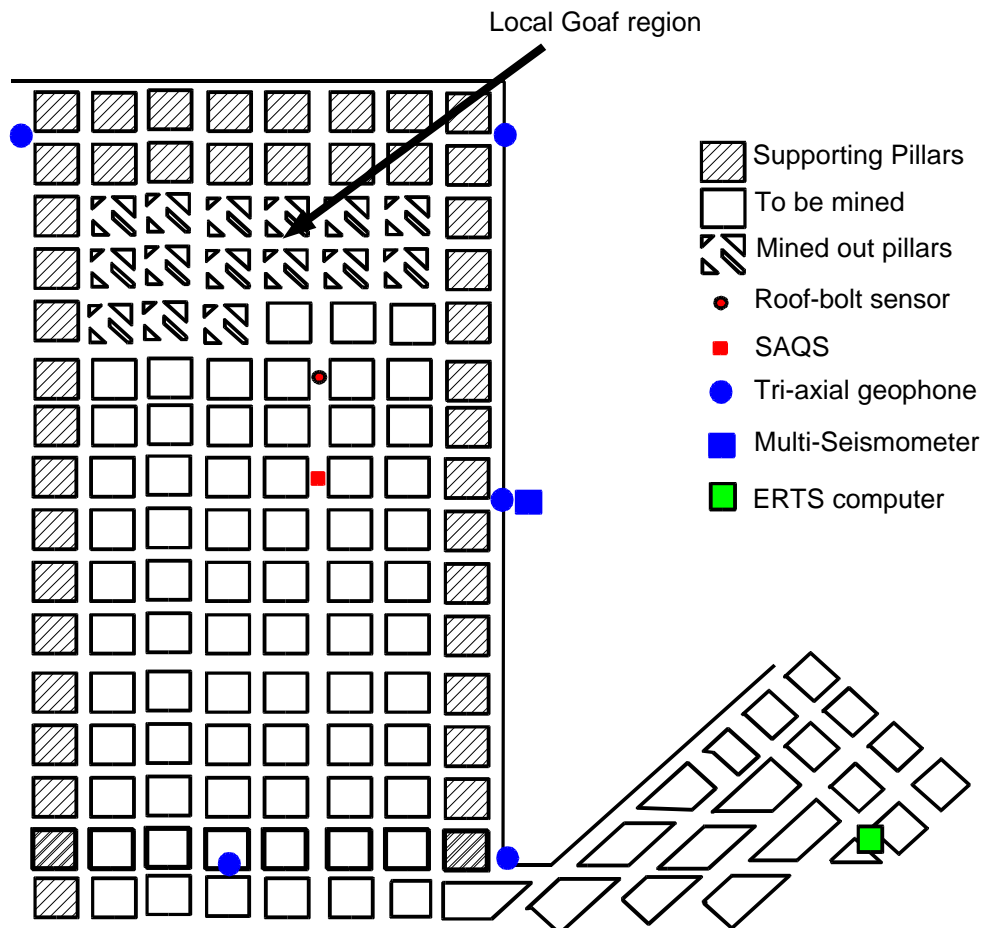


Figure 2: Configuration of the seismic network and roof-bolt geophone used in the project. As stooping proceeded from the top of the sub-section towards the bottom, the roof-bolt sensor and SAQS data logger were moved down to keep ahead of it. The seismic network did not have to be moved during the stooping of this sub-section.

The seismic network made use of mine-supplied electrical power. Since coal mining is a highly mobile operation, power disruptions are not uncommon. Consequently there are several time periods where data from the seismic network was not recorded. The Embedded Run Time System (ERTS) was set to record test-triggers every 2 hours. From this we can estimate the amount of time the system was recording seismicity. During the 20 days from the 3rd to 19th October, 119 test triggers were recorded out of an ideal 192. This indicates the network was recording for about 62% of the time. Figure 3 schematically indicates the periods when the seismic system was operational from the 3rd to the 19th October 2001.

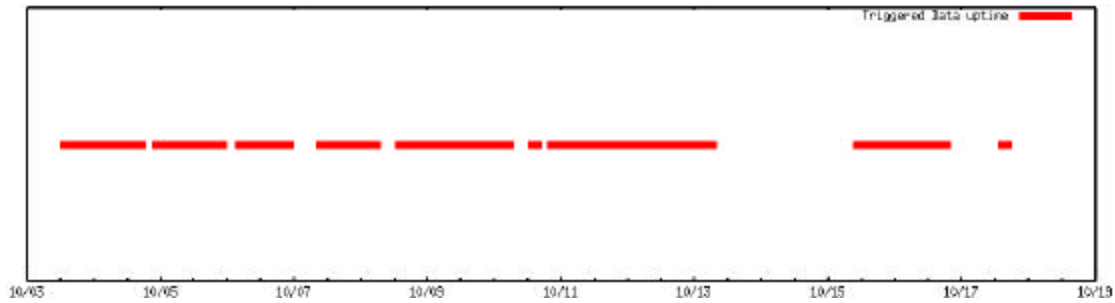


Figure 3: Graphical representation of the operational periods of the seismic network. Time is measured in days in October 2001 along the horizontal axis. Frequent power interruptions are common in coal mines, and are the cause of the periods of seismic network downtime.

The seismic signals from the 14Hz geophones were sampled at 8kHz, yielding a useful frequency bandwidth of 14-1600Hz. During the operational period 6,358 potential seismic events were recorded. After processing 2,257 events are accurately located and thus accepted. The recorded waveforms have dominant pulse frequencies of about 42G6Hz, with typical PPV amplitudes in the order of magnitude range 10^{-6} to 10^{-3} m/s. A typical seismic event recorded by the network is displayed below in Figure 4.



Figure 4: Tri-axial waveforms of a typical 3-station seismic event recorded by the seismic network. These waveforms exhibit clear P- and S-wave arrivals, with strong signal-to-noise ratios.

From the times at which recorded seismic events occur, seismic activity in each 15 minutes time interval over the 16 day period from the 5th to the 18th October 2001 may be derived. Such a graph is presented in Figure 5.

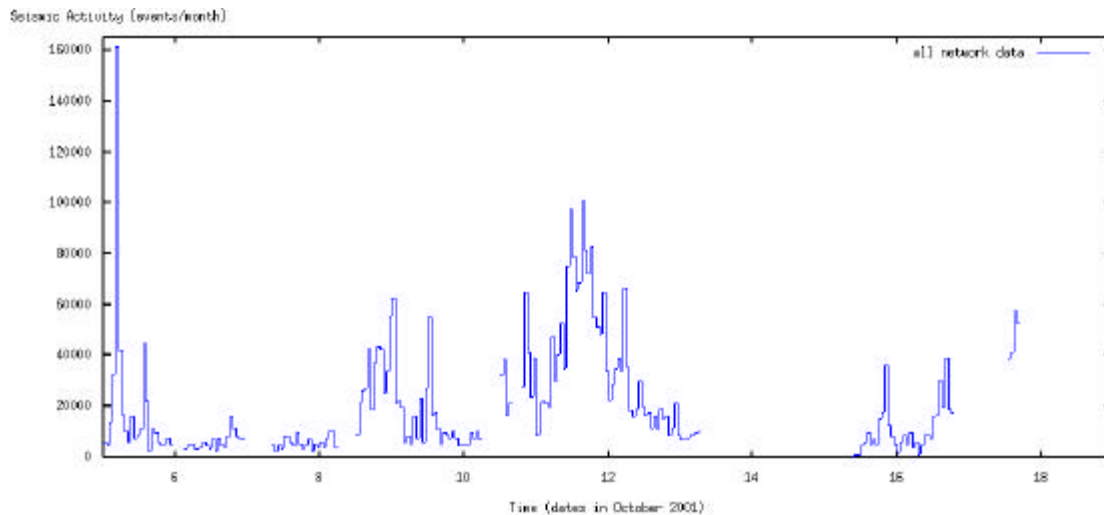


Figure 5. Seismic activity in section 17 as recorded by the network during October 2001. All recorded seismic events have been considered, and a time window of 15 minutes has been used to compute seismic activity.

For comparison, the seismic activity plot for the accurately located seismic event data recorded during COL607 is given in Figure 6. It is clear that recorded seismicity in section 17 was some 4-5 times higher than what was previously observed. This is due in part to the previous configuration of geophones -all on the one side of the stooping. This was necessary due to limited access. Clearly surrounding the stooping zone with sensors leads to higher sensitivity.

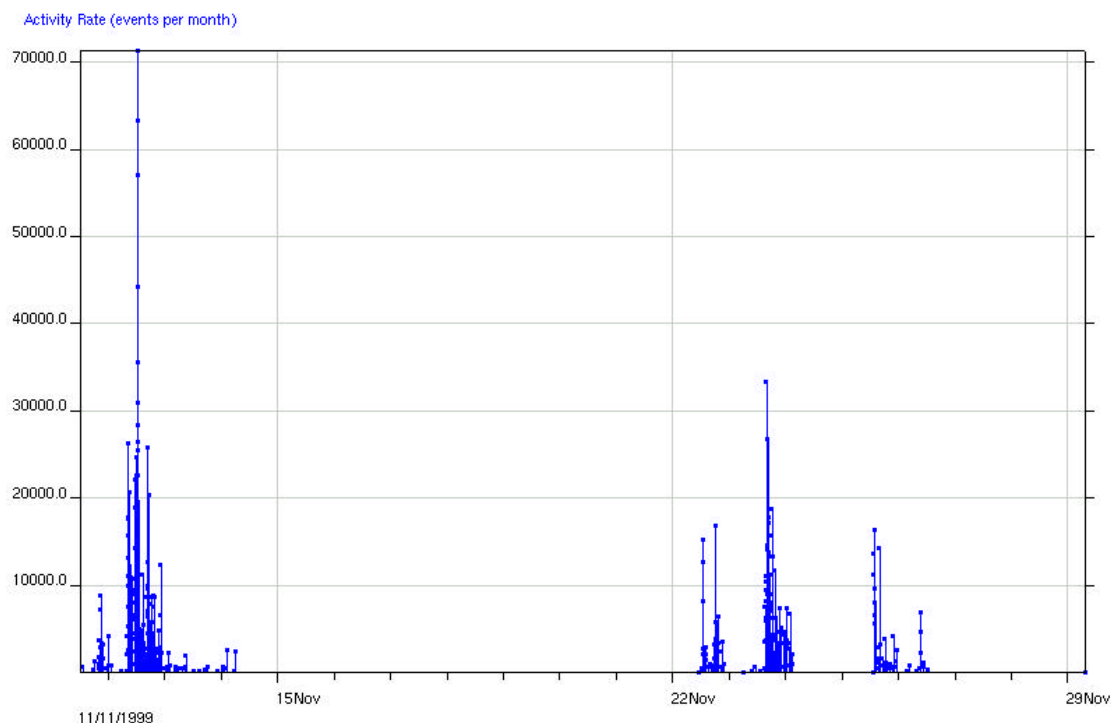


Figure 6: Seismic activity recorded by a temporary seismic network during COL607. This project concluded that seismic activity was the most reliable indicator of impending goafing

The Roof-Bolt Geophone

For this part of the project, a roof-bolt sensor had to be constructed. The sensor had to form good acoustic contact with the roof stratum, and so some kind of mechanism that clamped the geophone onto a standard roof-bolt had to be developed. Since this is the probable contact mechanism for any production version of a Counting Seismometer, a standard roof-bolt stub found in Brandspruit #2 is shown in figure 7.



Figure 7: Standard roof-bolt stub found in Brandspruit #2. The length of stub protruding beyond the nut is approximately 30mm. Many of these bolts are installed in a mining area, and are thus perfect for connecting the seismic sensor to, providing no detailed waveform analysis is required.

A tri-axial 30Hz geophone was manufactured to tightly grip the stub of the roof-bolt. This arrangement proved convenient and quick to install and remove, and is recommended for any future work. The sensor was tested and approved for a methane environment by the SABS explosion prevention department.

Seismic signals from the roof-bolt geophone were carried via instrumentation cable and barriers to a Stand-Alone QS (SAQS) data logger. The SAQS is capable of continuously logging seismic signals to a removable Firewire hard disk for later download and interpretation. Sampling rates of up to 24kHz are possible. Since any future Counting Seismometer would use only a single vertically oriented geophone component with relatively low sampling rate, it was decided to sample the vertical component of the roof-bolt geophone continuously at 3kHz. A sharp sigma-delta filter within the SAQS yields an effective upper frequency limit of 1350Hz. The lower limit is determined by the geophone, about 30Hz in this case.

The SAQS is not intrinsically safe and so had to be fitted into a small flame-proof enclosure, of mass approximately 50kg. The SAQS and enclosure are shown in Figure 8.

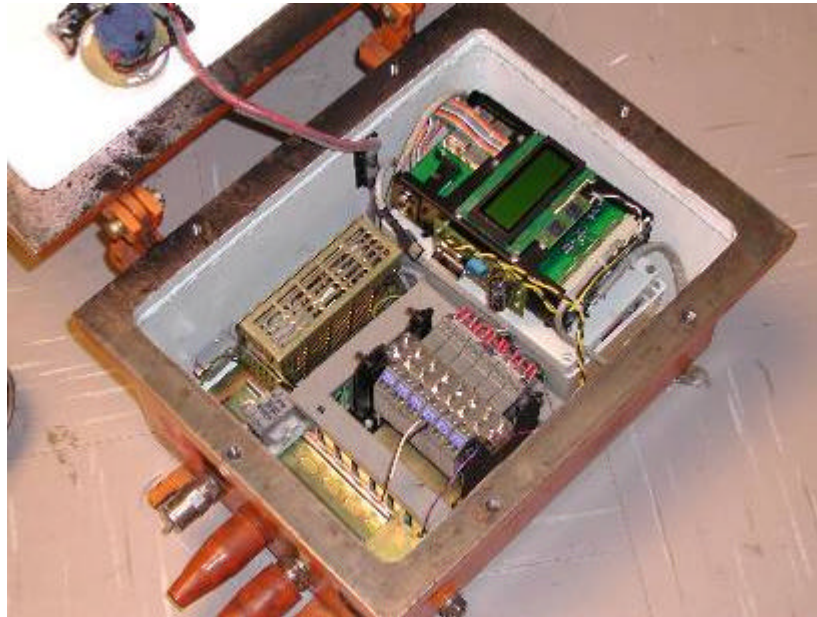


Figure 8: StandAlone QS mounted within a flame-proof enclosure for use in a possible methane environment. The enclosure could be moved by one person and was thus relatively portable in the mining environment.

The SAQS and roof-bolt geophone were pulled back every couple of days to keep ahead of the stooping operations. The data logger was powered from the switch-cart 220V source. As with the network, power interruptions were common. At 3kHz sampling rate, a seismogram should be recorded every 8.4 seconds - some 10,286 per day. Between the 5th and the 19th October 2001 there were 106,523 seismograms recorded, out of a theoretical 164,571. This implies that the SAQS data logger was operational for about 65% of this period. Since each seismograms should immediately follow the previous one, it is easy to determine the exact times at which the system was shut down and started up. This information is represented in Figure 9.

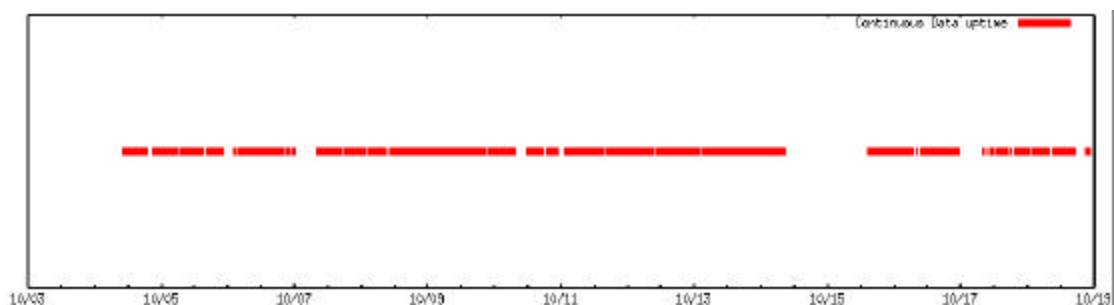


Figure 9: Graphical representation of the operational periods of the roof-bolt system. The StandAlone QS recorded continuous seismic signals from the roof-bolt geophone for about 65% of the monitoring period.

Most of the recorded seismograms (about 95%) are featureless noise. An example is shown in Figure 10. The noise is Gaussian in nature, with standard deviation of about $8.6 \times 10^{-7} \text{ m/s}$. This leads to a theoretical Long Term Average (LTA) of 2×10^{-3}

Z 5.7×10^{-7} m/s. The character of the noise is consistent with the electronic noise levels of the acquisition electronics.

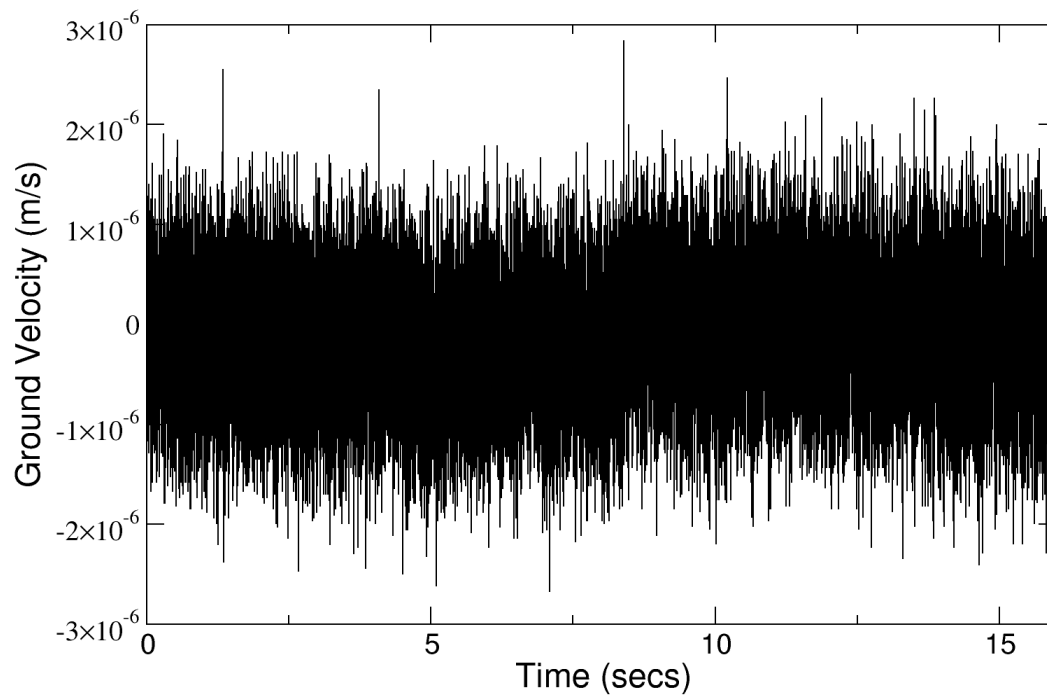


Figure 10: Most of the continuous seismic signal from the roof-bolt geophone consists of featureless noise like this.

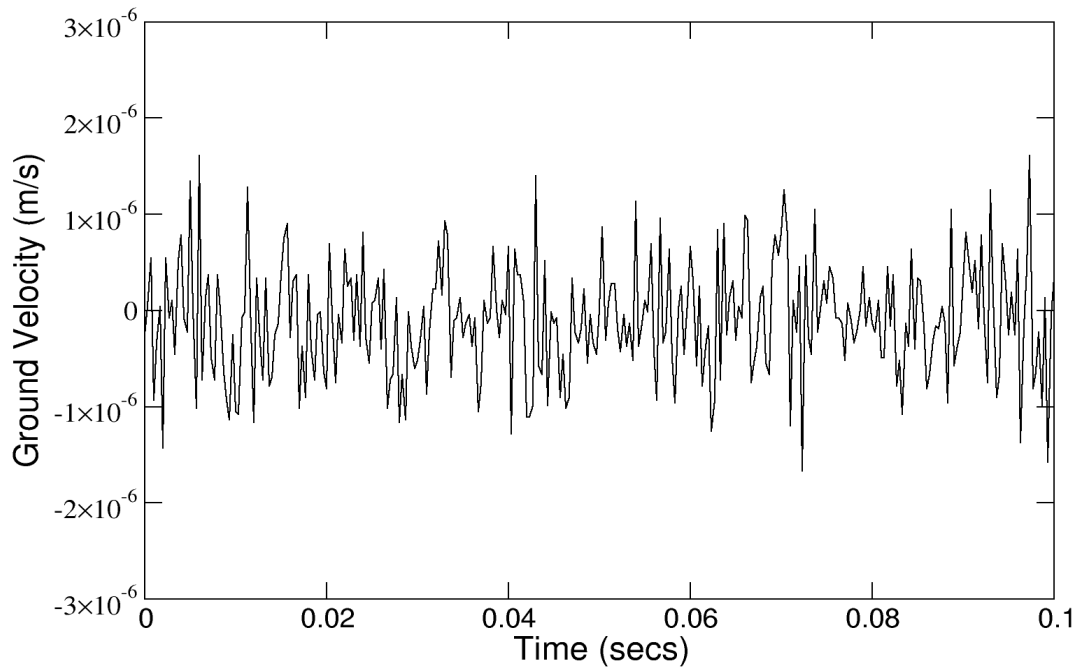


Figure 11: Expanded time section of Figure 10, above. The signal is thermal in origin and thus exhibits a frequency-dependant power spectrum with most of the power in the low end.

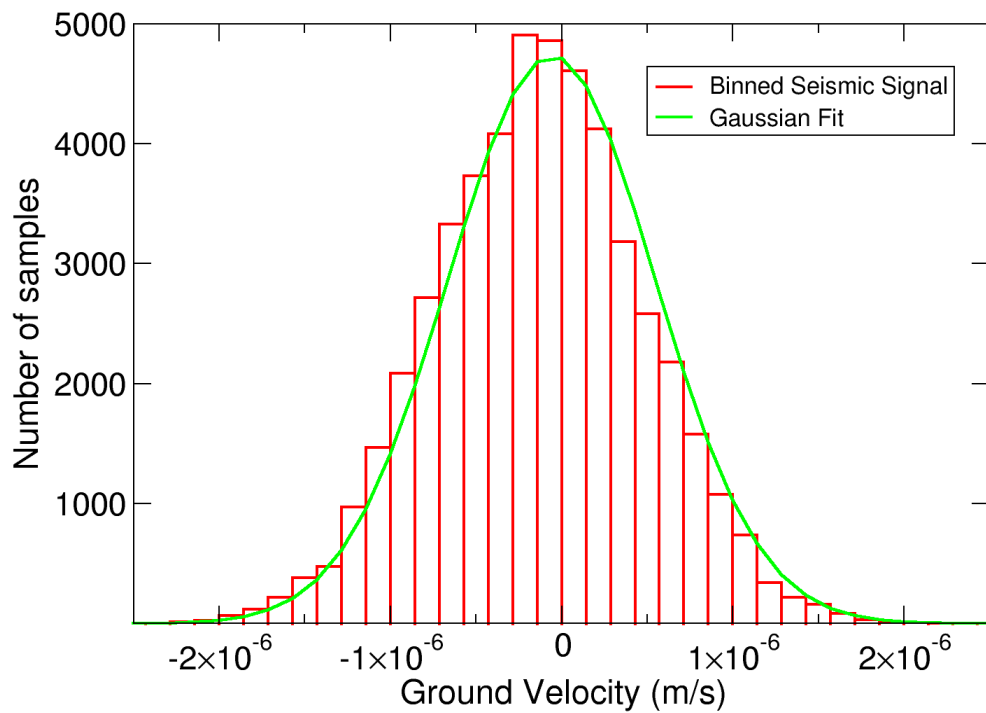


Figure 12: An analysis of the signal statistics reveals a simple Gaussian structure with a standard deviation of 8.6×10^{-7} m/s.

Interesting seismic signals occasionally rise out of the background. These signals have 2 possible origins: fracturing of the rock mass by mining-induced stresses or signatures of mechanical mining. An example of mining noises is given in Figure 13.

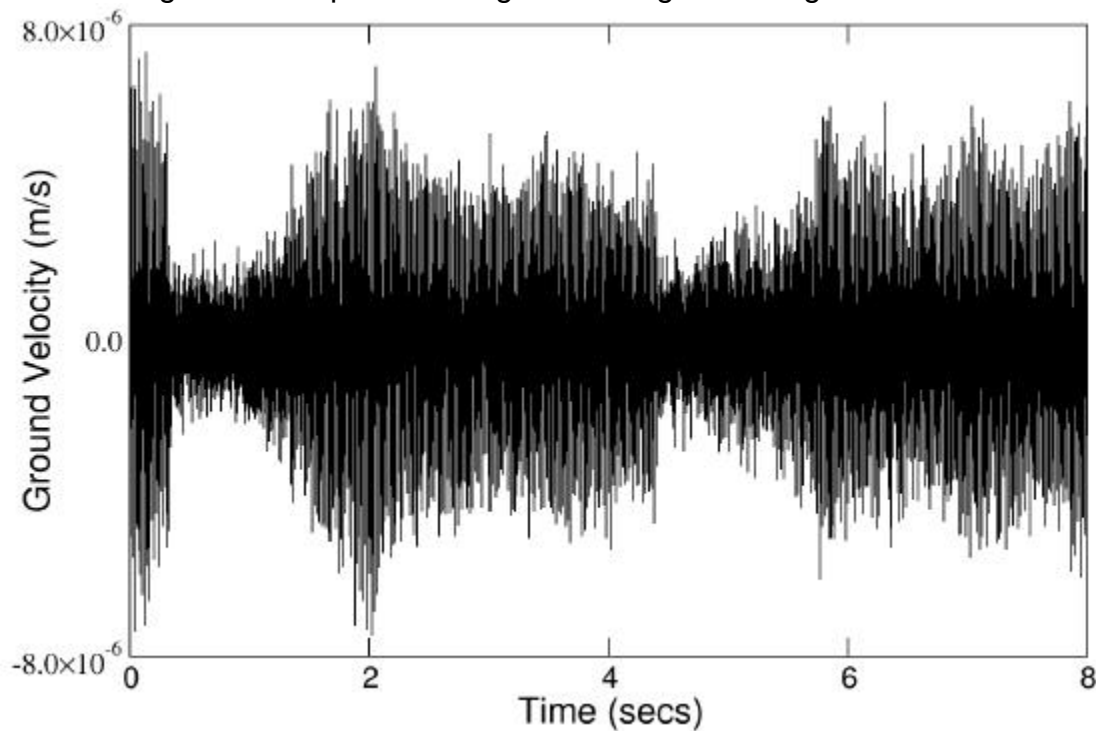


Figure 13: An example of mining seismic signals. Our Counting Seismometer should not regard this kind of signal as increasing seismic activity.

It becomes clear that the signal in Figure 13 is man-made when regarding a small time segment of it (Figure 14). Clearly the signal has dominant periodicity not found in fracture-generated seismograms. A Fourier transform reveals the predominant 50Hz power common in electrical equipment in South Africa - see Figure 15.

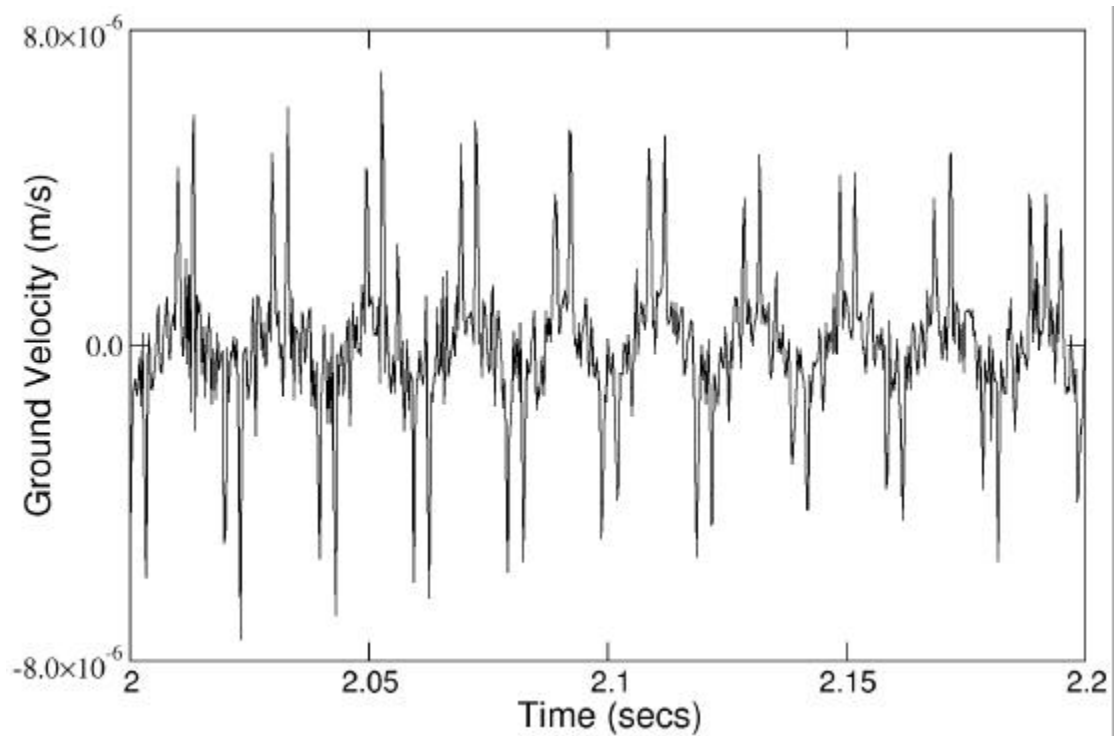


Figure 14: Small time segment of Figure 13. Clear periodicity is apparent, unlike in signatures of rock fracturing. The Counting Seismometer algorithm must be able to distinguish between these kind of man-made noises and genuine seismic events.

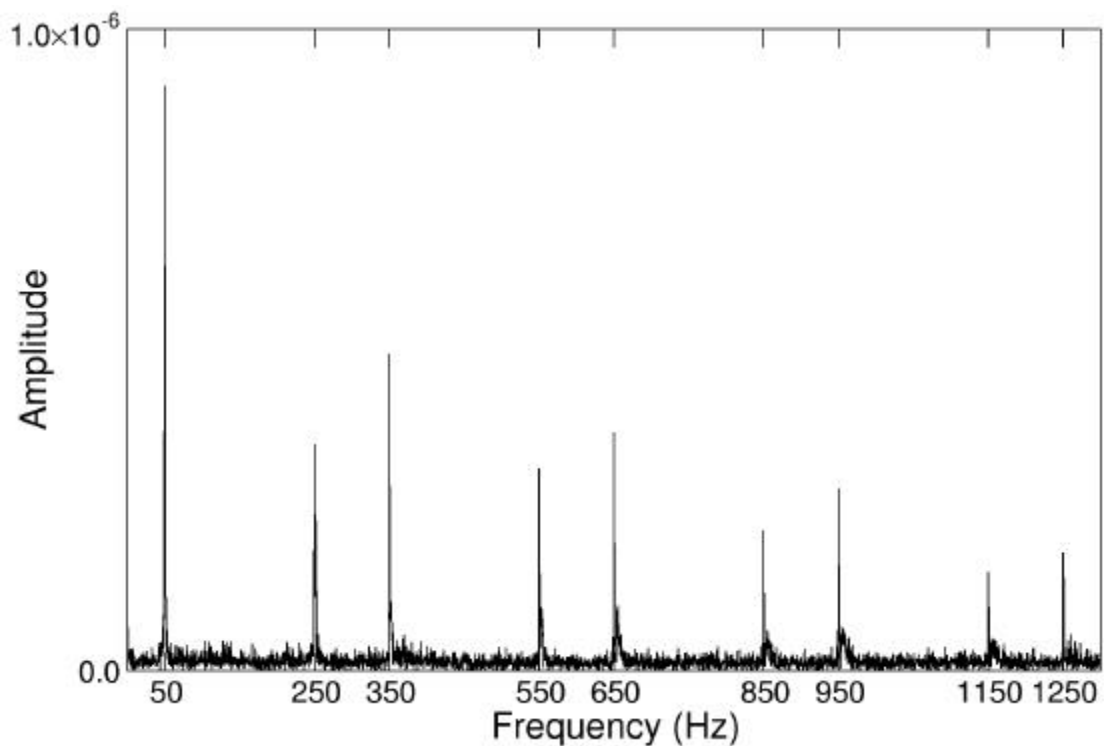


Figure 15: Fourier transform of the signals of Figure 13. A 50Hz dominant frequency suggests the noise has an electrical origin in South Africa - possibly this signal is electrically induced in the geophone cable and is not a vibration at all.

This kind of 50Hz dominated signals are probably caused by electrical interference - perhaps the cable feeding current to the Continuous Miner was routed alongside the sensor cable at this time. This kind of signal is not very large in amplitude and should not be recorded by a Counting Seismometer, since this device will not have the long cables between the geophone and the digital-to-analogue converter that act as antennae for induced signals.

Another type of obvious machine noise is shown in Figure 16. This noise is stronger in amplitude and lacks any discernible periodic components, as seen in the expanded Figure 17.

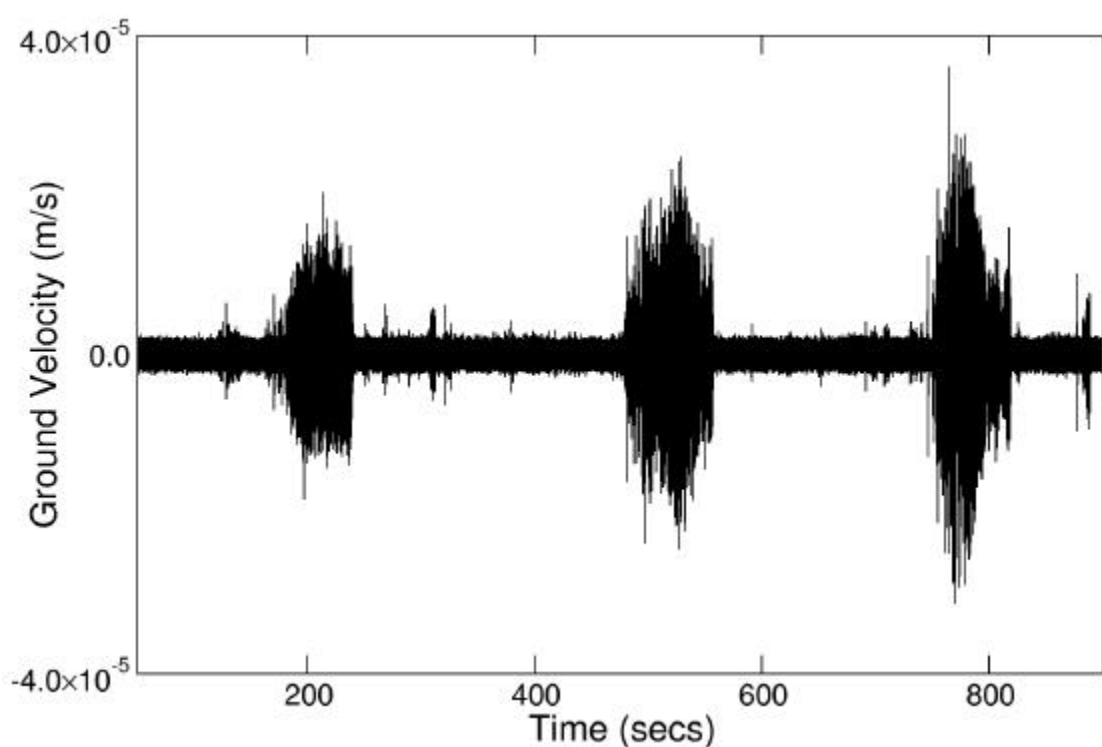


Figure 16: Another kind of obvious machine noise recorded by the roof-bolt geophone. Any useful Counting Seismometer algorithm needs to ignore these kind of signals.

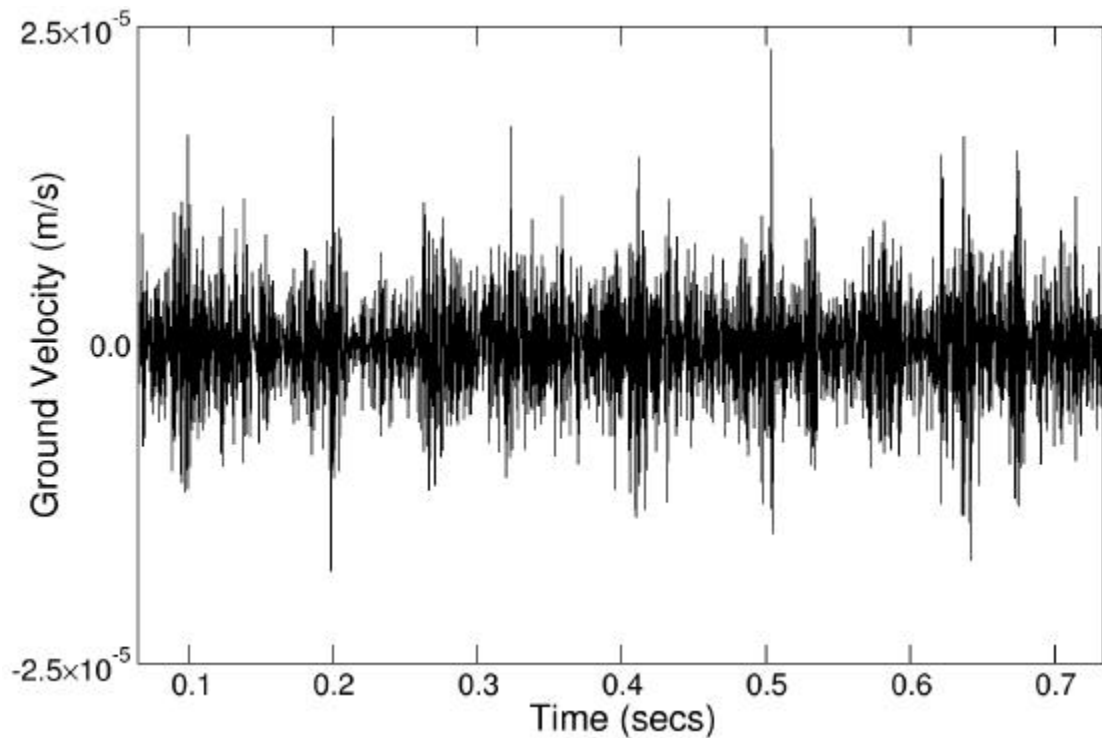


Figure 17: An expanded time section of the middle burst of noise of Figure 16. No dominant frequency is obvious.

The source of this man-made noise is probably the Continuous Miner. At this time the CM was operating about 60-70m away from the roof-bolt sensor. The LTA of this signal, defined by

$$LTA = \frac{1}{N} \sum_{i=1}^N s_i$$

is 1.4×10^{-6} m/s, or about 2.5 times the normal background noise levels.

In amongst the machine noises and rising above the background are signals which look very much like signatures of fracturing. An example is given in Figure 18. These signals are very much shorter than machine noises, typically some hundreds of milli-seconds in duration, and of Peak Particle Velocity (PPV) in the order of magnitude ranges 10^{-6} to 10^{-3} m/s.

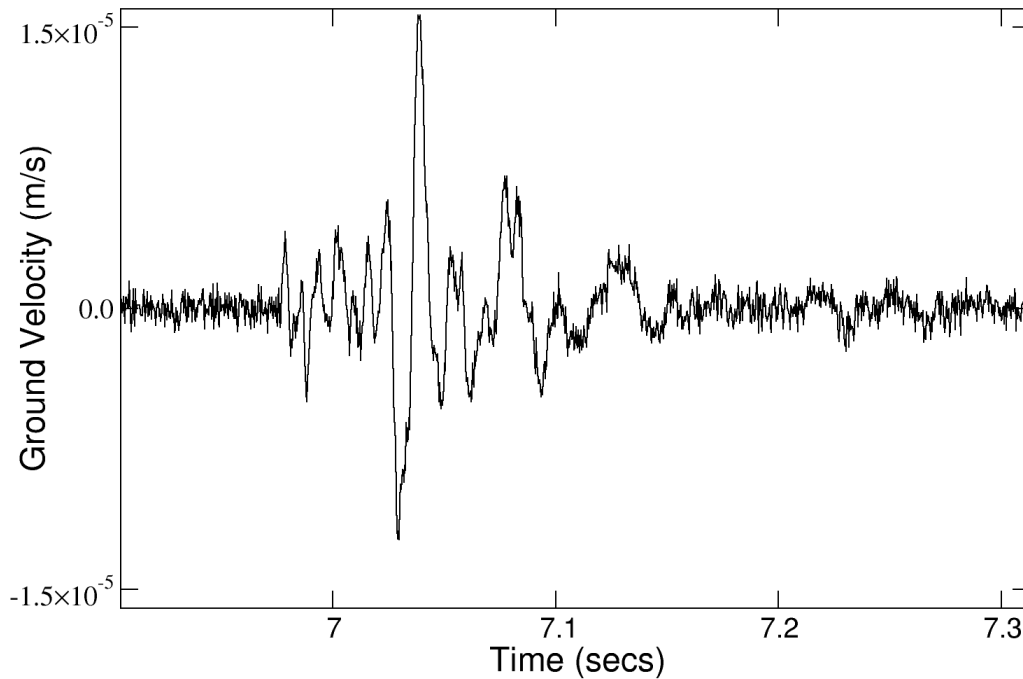


Figure 18: Example of a likely rock fracture-like signal. P- and S-wave arrivals may be discerned, although difficult to confirm with a single component.

It is interesting to consider the average ground motions over subsequent 100 second intervals. Here we see that intermittent bursts of machine activity raise the background noise levels by factors of less than 10 for a roof-bolt sensor sited between 50m and 120m away. Each burst lasts some hundreds of seconds.

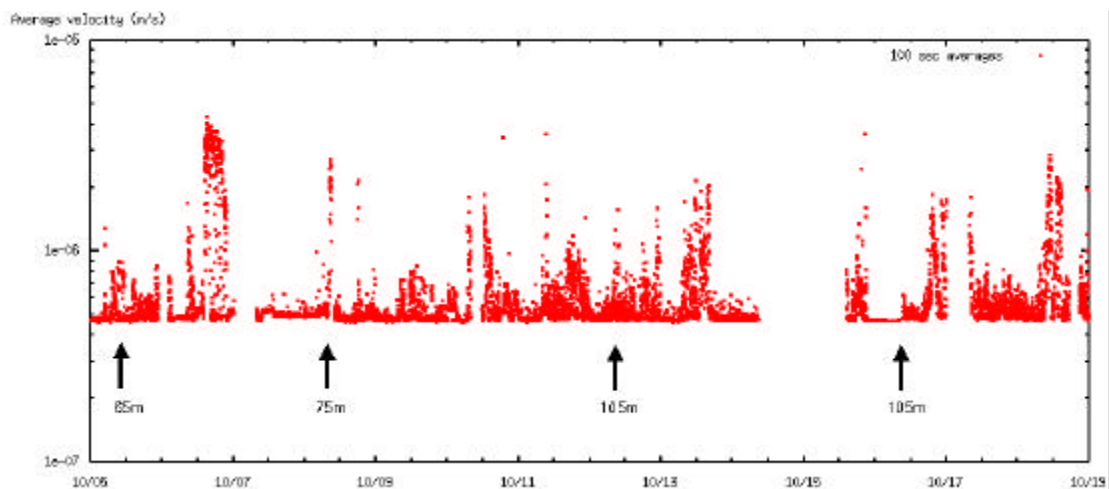


Figure 19: Average ground velocities for 100 second intervals during the monitoring period in October 2001. Arrows and distances refer to the distances between the roof bolt geophone and the Continuous Miner at those times.

Triggering Algorithms

Ultimately this project aims at finding a triggering algorithm that will count a well-behaved waveform (e.g. Figure 18) as a "real" seismic event and ignore waveforms caused by mining machinery (e.g. Figures 15 and 16). The algorithm must be as simple as possible in order for it to run on a small low-power micro-processor.

Fixed Level Triggering

The simplest possible form of triggering is fixed level triggering. Here a pre-set level is defined and as soon as the seismic signal exceeds this threshold, an event is triggered. Care has to be taken in removing any DC offset from the signal. The most complicated part is knowing when to de-trigger. Clearly the many swings of a seismogram should not be recorded as individual events. This may be accounted for by only de-triggering when a certain number of subsequent samples are below the threshold. The major disadvantage of the method in this setting is that when machinery is operating and the background noise level rises the algorithm can be in a perpetual trigger state until the noise stops. During this time the Counting Seismometer would be deaf to any larger seismic signals that rise out of the noise. Simply raising the trigger threshold to sit above any possible machine noise is one solution - one can see in Figure 19 that a threshold of about 10^{-5} m/s would do the trick. However in this case smaller fracture signals during periods of quiet would be ignored.

STA/LTA

A common triggering algorithm in seismic monitoring is the Short-Term-Average (STA) Long-Term-Average (LTA) method. Here the STA/LTA ratio is monitored, and an event is triggered when this ratio exceeds a pre-defined trigger ratio. The most memory-efficient way of implementing this is by the formulae:

$$STA_i = \frac{1}{N_{STA}} \sum_{j=1}^{N_{STA}} x_{i+j-1}$$

$$LTA_i = \frac{1}{N_{LTA}} \sum_{j=1}^{N_{LTA}} x_{i+j-1}$$

The length of the STA is usually 16 samples, while the LTA length is something like 50,000. A common trigger ratio set in the ISS systems is a factor 8.

The major advantage of this method over fixed level triggering is that the effective sensitivity lowers during periods of high background noise and increases when the noise drops.

The disadvantage of STA/LTA triggering in the coal mine environment is that the bursts of machine noise are sometimes not continuously high signals, but consist of a series of

impacts. Each of these impacts would count as a "real" fracture event. See Figure 20 and the time expansion in Figure 21 for an example.

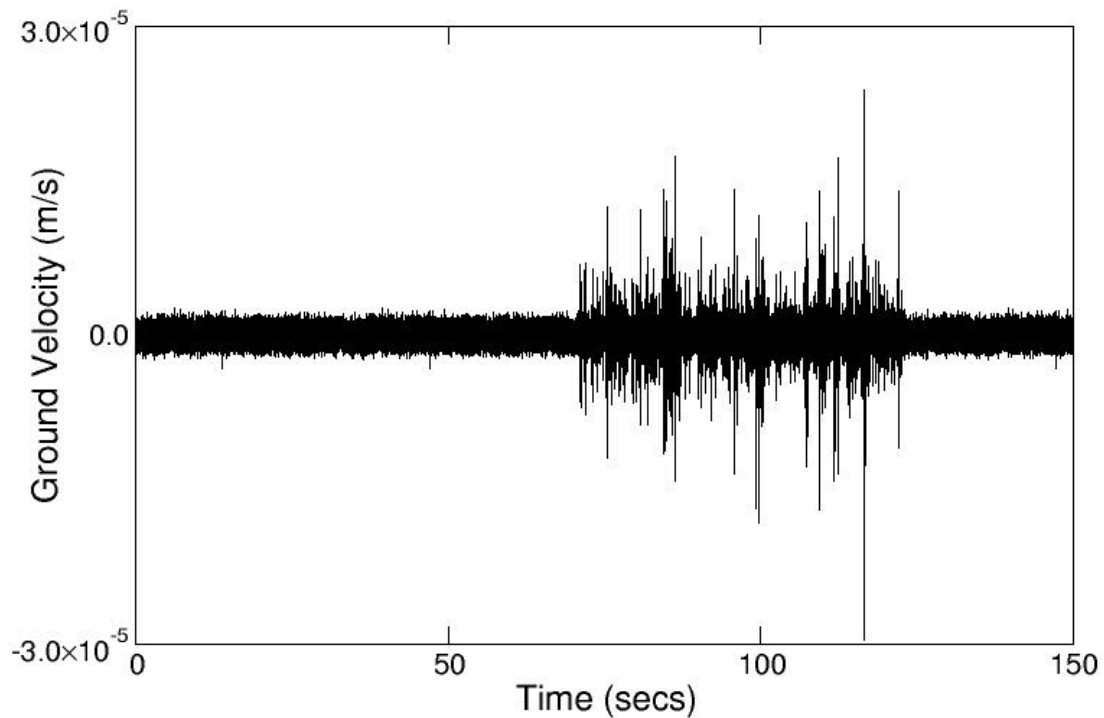


Figure 20: A typical burst of machine noise recorded by the roof-bolt sensor. The beginning of the burst is expanded in Figure 21.

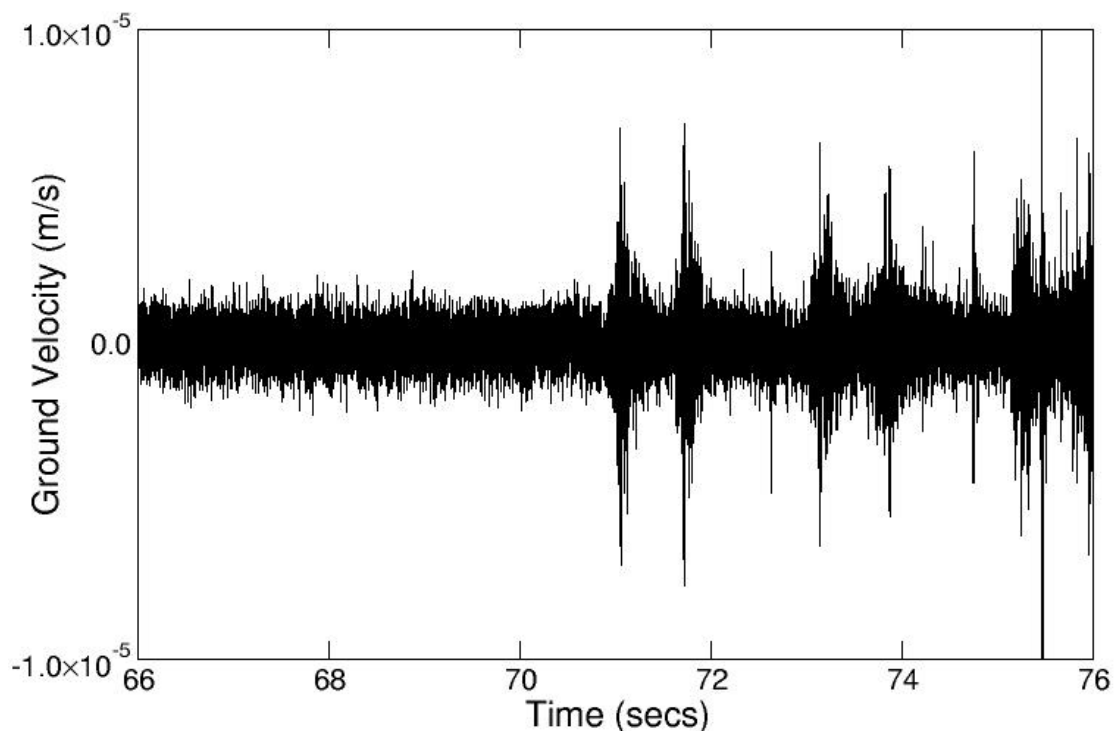


Figure 21: Time expanded view of the beginning of the machine operation shown in Figure 20. Each of the individual events would trigger an STA/LTA algorithm.

It is true that the LTA rises during this burst of machine noise, but this is slow and so the first few individual events satisfy the STA/LTA triggering criterion and are counted. If the LTA is made shorter, then it rises faster but also decays faster. This can mean that many single events in the machine burst can be incorrectly counted. In addition, large low frequency events can be ignored if the LTA is too short. The STA (length 16) is given for the burst of machine noise - Figure 22. Then both a short LTA of length 2000 and a longer LTA of length 20000 is shown for this time period in Figure 23. The initial events trigger the STA/LTA₂₀₀₀₀ algorithm because the LTA cannot rise fast enough. This is a problem given how often the machines switch on and off.

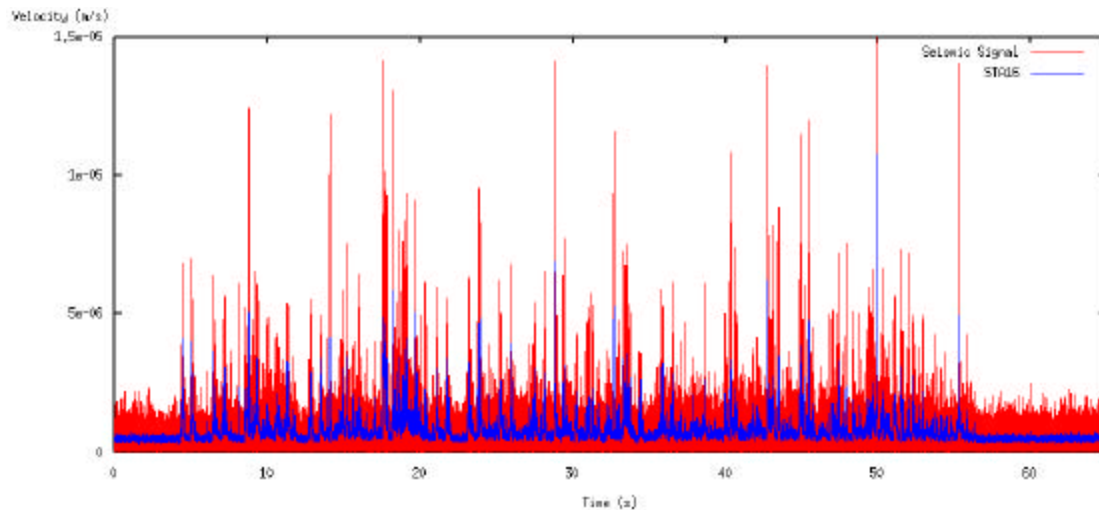


Figure 22: Seismic signal of the burst of machine noise and the effects on a Short-Term-Average of length 16.

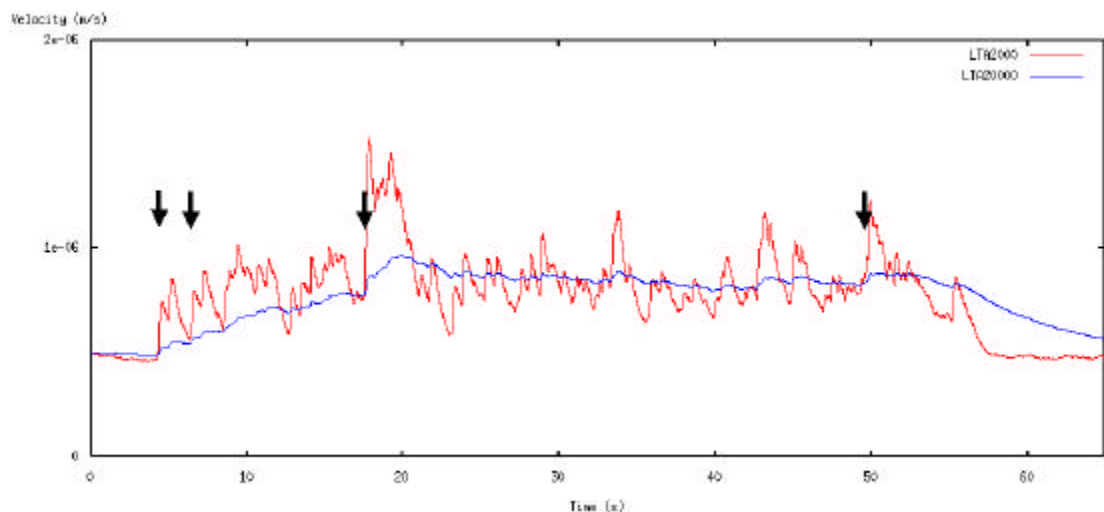


Figure 23: Effects of the seismic signal in Figure 22 on a Long-Term-Average of length 2000 and one of length 20000. The arrows indicate where the STA/LTA₂₀₀₀₀ criterion would trigger, and incorrectly regard this burst of machine noise as an increase in seismic activity.

Asymmetric LTA's

The LTA2000 / LTA20000 figure (Figure 23) shows that one cannot have an LTA that both rises quickly and stays constantly high during the machine noise. The answer is to break the symmetry of the LTA calculation in such a way that the rises are rapid and the decays slow. This may be achieved by using a different LTA length depending on whether the next rectified sample is greater or less than the present value of the LTA. Obviously a bias is introduced, but this is easily accounted for.

Using values of 2000 and 20000 for the two LTA lengths, we obtain Figure 24. Here we see that the LTA has risen high enough to remove one of the incorrect triggers. However 3 triggers remain.

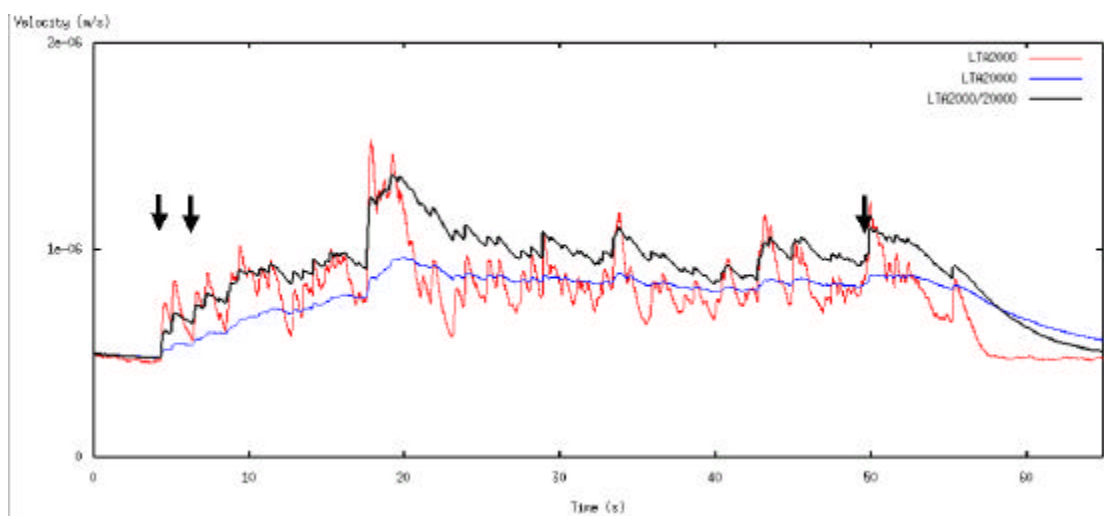


Figure 24: Symmetric LTA's of length 2000 and 20000 with an asymmetric LTA of lengths 2000 and 20000 are shown for the burst of machine noise. Note how the asymmetric LTA rises as quickly as the shorter LTA but rises consistently even higher than the longer LTA.

The asymmetric LTA is as easy and memory-efficient as a normal LTA, but the initial triggers at the start of the machine noise is still a problem.

Delayed Validation

One would ideally like to know in advance if the LTA is going to rise substantially, i.e. If a period of sustained noise is starting. Fortunately the decision can be made retrospectively some tens of seconds after triggering, since this delay should not be critical. The algorithm is then:

1. Trigger using STA-asymmetric LTA criterion, and begin counting down a timer
2. While the event is triggered, determine the maximal STA
3. De-trigger normally, but wait for the timer to finish before deciding about the event
4. As the timer elapses, compare the maximal recorded STA with the LTA at the present

time. If the STA/LTA criterion is still met, accept the event as legitimate.

Effectively, this method is conditional on both signal before the event (the LTA at the time of triggering) and the signal after the event (the LTA some time later). If the LTA is the same at both these points, then the event has risen above the noise and should be accepted. If the LTA is low initially and then becomes large, then probably sustained machine noise is being monitored. If the LTA is high initially and becomes low, then the machine noise is ending. Since the event was large enough to rise above the noise and trigger initially, it should be accepted.

Figure 25 shows how this approach removes the first 2 spurious triggers. The last trigger occurs despite a high LTA level and therefore should be accepted. In retrospect, it seems impossible to judge this last trigger as false or genuine.

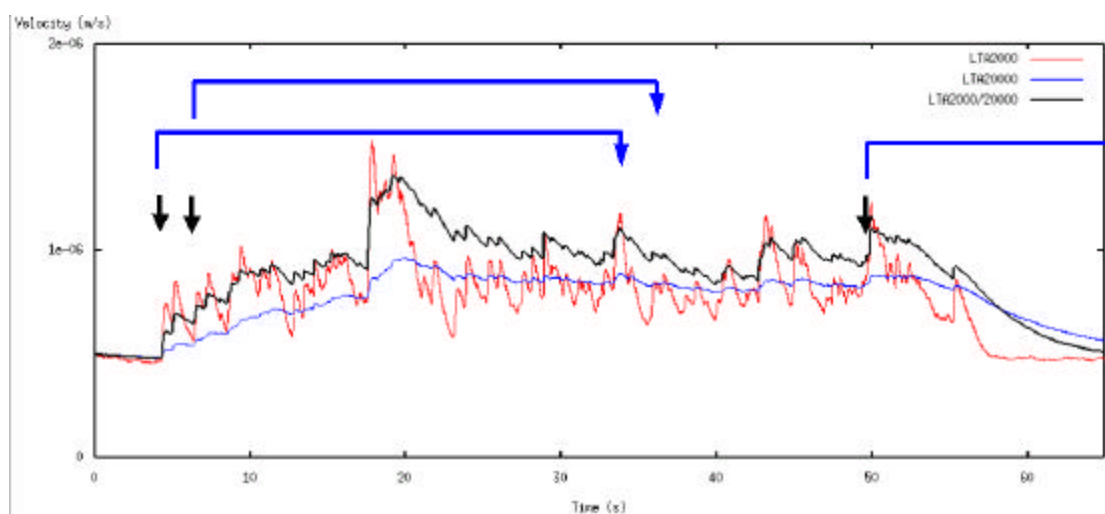


Figure 25: The delayed validation approach combined with the asymmetric LTA filters out the spurious triggers at the beginning of the machine noise. The trigger towards the end of the machine noise is accepted as a probable signature of fracturing.

Comparisons between the Network and Roof-Bolt Data

Before we can begin to compare the seismic event data recorded by the ERTS network with the continuous data yielded by the SAQS we must determine the time differences between the 2 data loggers. This time difference is expected to be small, or the order of minutes. Finding common seismic events in the two records proved non-trivial, and so a more sophisticated approach was required.

On the 8th October 2001, the ERTS network recorded 593 seismic associations. Of these, 248 are accepted as legitimate seismic events after processing. On the same day the roof-bolt SAQS recorded 534 seismograms with interesting signals that rise out of the noise. We wish to find the time difference between the two sets of data that maximises the number of events recorded simultaneously by the two seismic data loggers:

$$P(\hat{O}t) = \frac{1}{248} \sum_{i=0}^{248} \sum_{j=0}^{534} \hat{E}(\zeta t - B_{s_i} - B_{T_j} - \hat{O}t) \quad \text{The length of the time window within both events}$$

must fall to be counted, ζt , was set to 2 seconds in this exercise. The Heavyside step function \hat{E} has it's usual meaning here, being equal to unity with a positive argument, and zero otherwise. A graph of $P(\hat{O}t)$ vs $\hat{O}t$ is given in Figures 26a & 26b. Evidently an offset of -45s between the network and roof-bolt data gives the best correspondence of about 50%. This means that at this offset about 50% of the network events are evident in the SAQS data.

One would expect that the roof-bolt geophone would record all network events and more. However there are several reasons why this is not the case. Firstly the geophones are different. The 14Hz geophones of the network have a greater sensitivity (28.8V/m/s as opposed to 11.0V/m/s) as well as a lower frequency limit. Indeed the network events recorded by the roof-bolt sensor have an average PPV of 5.1×10^{-5} m/s, whereas the events missed by the roof-bolt have an average PPV of 2.6×10^{-5} m/s. Furthermore there are site-specific details like the fractured nature of the roof stratum in the middle of the stooping sub-section compared with the roof condition closer to the edges.

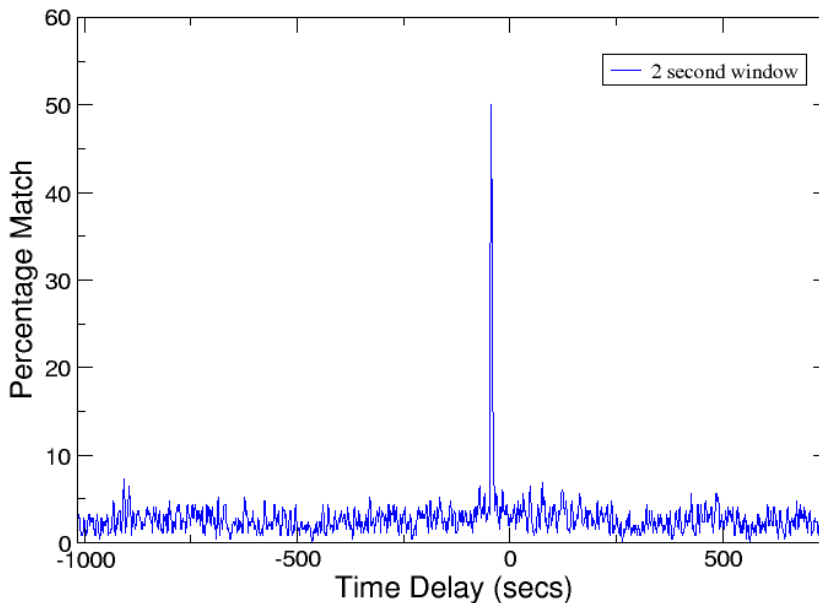


Figure 26a: Percentage of network events that are evident in the roof-bolt continuous data as a function of the time offset between the two datasets.

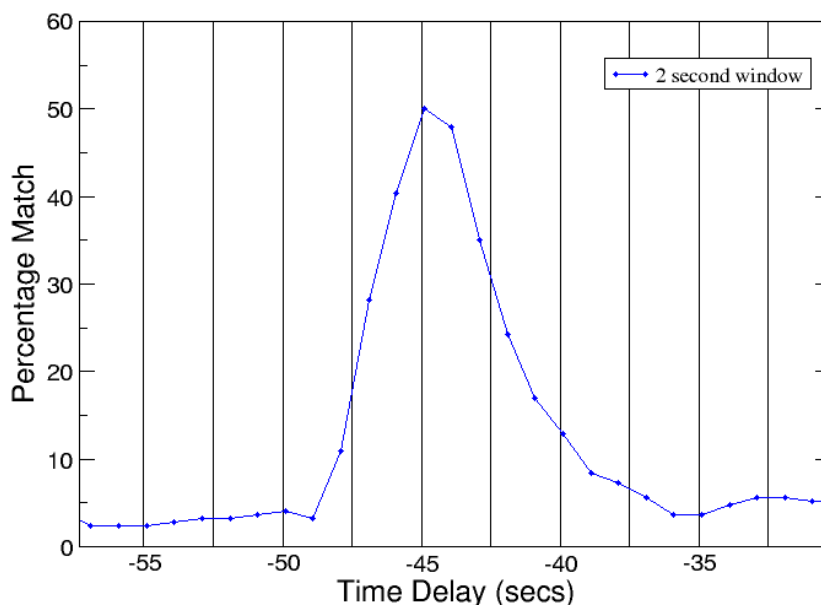


Figure 26b: Expanded view of the peak percentage match shown in Figure 4a. The network and roof-bolt data is most concordant at a time offset of 45 seconds. At this off-set about 50% of the seismic data recorded by the roof-bolt geophone and the seismic network is common.

The most sensible manner of determining the extent to which the Counting Seismometer triggering algorithms produce data similar to the network data is by means of comparing relative seismic activity. An STA/asymmetric LTA criterion with parameters given in Table 1 triggers 10997 times during the 16 days from 5th to 18th October 2001. Recall that during this time the SAQS was only recording for 65% of the time. Of these 10,997 events, 836 events (7.6%) are rejected by the delayed validation scheme.

| STA length | LTA length (-) | LTA length (+) | Timer length |
|-------------------|-----------------------|-----------------------|---------------------|
| 16 samples | 20,000 samples | 2,000 samples | 90,000 samples |

Table 1: Counting Seismometer algorithm parameters used for trigger extraction from continuous roof-bolt data

The seismic activity in time windows of 15 minutes for the 16 day period from 5th to 18th October 2001 is presented in Figure 27. Only time windows for which both data loggers were operational are considered here. All network data is used to compute the seismic activity.

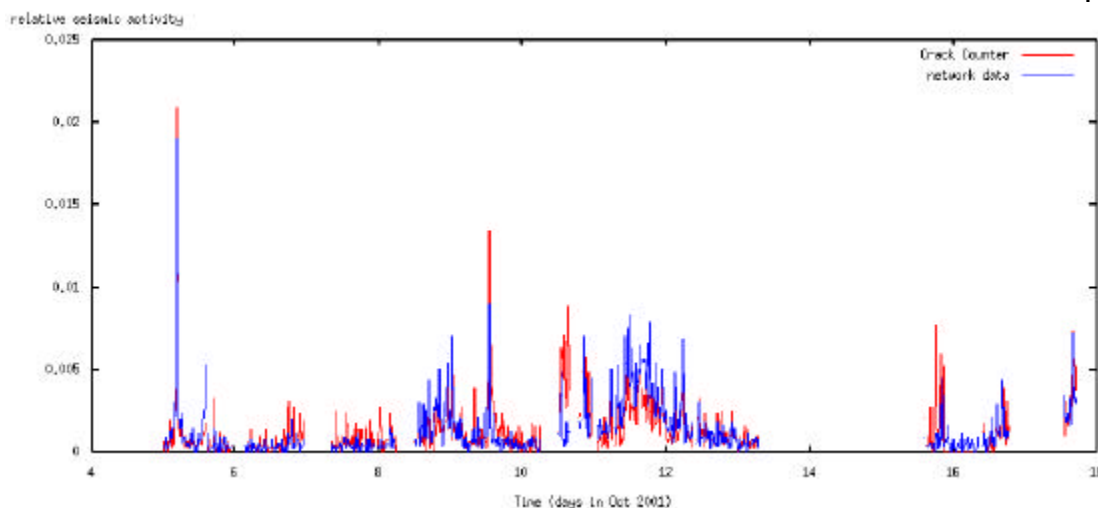


Figure 27: Seismic activity for the Counting Seismometer data and the data recorded by the seismic network. A striking similarity is apparent, indicating the strong feasibility of a successful routine Counting Seismometer.

The correlation between the two activity time series may be quantified by a correlation function:

$$Corr_{cc,net} = \frac{\sum_{i=1}^N cc_i \cdot net_i}{\sqrt{\left(\sum_{i=1}^N cc_i^2\right) \left(\sum_{i=1}^N net_i^2\right)}}$$

where cc_i and net_i are the Counting Seismometer and network activities in the i^{th} time interval, respectively. A value of 1 indicates perfect correlation, while zero indicates uncorrelated behaviour. The value of the correlation differs with choice of time interval length; some values are given in table 2.

| Time Interval | Correlation - no delayed validation | Correlation - delayed validation |
|----------------------|--|---|
| 5 min | 68.7% | 69.0% |
| 15 min | 74.6% | 74.8% |
| 30 min | 76.5% | 76.8% |
| 60 min | 76.8% | 77.2% |

Table 2. The seismic activity computed from all recorded network data is compared with activity computed from the Counting Seismometer algorithm, both with and without a delayed validation mechanism.

Correlations of between 70% and 80% are very pleasing, especially with such a simple triggering algorithm. Unfortunately the area did not experience any significant goafing during the project, contrary to all expectations, and so we do not have precursory activity

data to compare against. Since ISSI personnel had to remain on site at all times to keep the system operational (moving the roof-bolt sensor and checking everything after power interruptions), it was outside of the budget to extend the monitoring period in the hope of recording the goaf.

COL607 showed that seismic activity recorded by a network was helpful in anticipating goafs. Since there is no reason why the correspondence will not extend to this domain, it is believed that the Counting Seismometer algorithm will perform satisfactorily.

Counting Seismometer Requirements

The algorithm has been investigated and is certainly simple enough to run on a small micro-processor. Any envisaged Counting Seismometer should be very small (hand-sized) and be mounted on roof-bolt stubs, which are plentiful in the stooing area. The unit should be battery powered, and last some weeks between battery refreshes. Use of a 30Hz geophone should allow the Counting Seismometer to be omni-directional and eliminate the need for any levelling mechanisms. A moving time window should be used to compute seismic activity, and there should be a facility for setting the activity level at which an alarm is raised. This alarm could be by means of flashing lights and high-pitched piezo-electric buzzers. The cost should be low enough so each stooing section could use a few of these devices.

Conclusions

The experimental part of the project proceeded according to plan, with the exception of the absence of major goafing during the seismic monitoring. Equipment manufacturing, intrinsic safety certification, system installation and commissioning, operating and final de-commissioning were all satisfactory.

The uni-axial geophone record has revealed that a simple triggering algorithm can produce similar data to that which is recorded by a network of 5 tri-axial geophones. This result paves the way for development of a small portable device that monitors local seismicity and warns of increasing activity. Technically this is not a rigorous challenge, and thus this project may be regarded as having achieved it's goal of establishing the feasibility of the Counting Seismometer concept.

References

COL607 - SIMRAC research project conducted by ISS International (Dr W de Beer) during 1999-2000.

GUIDE1999 A J Mendecki, G van Aswegen & P Mountfort, *A Guide to Routine Seismic Monitoring in Mines* - in *A Handbook on Rock Engineering Practice for Tabular Hard Rock Mines*, A J Jager and A J Ryder (Eds).

A J Mendecki, *Quantitative seismology and rockmass stability*, in *Seismic Monitoring in Mines*, A J Mendecki (Ed.), Chapman and Hall, Cambridge, 1997.